



# HHS Public Access

Author manuscript

*Colloids Surf A Physicochem Eng Asp.* Author manuscript; available in PMC 2017 February 08.

Published in final edited form as:

*Colloids Surf A Physicochem Eng Asp.* 2016 September 5; 504: 305–311. doi:10.1016/j.colsurfa.2016.05.085.

## Pendant-drop method coupled to ultraviolet-visible spectroscopy: A useful tool to investigate interfacial phenomena

Marco A.R. Andrade<sup>a</sup>, Bruno Favarin<sup>a</sup>, Rafael Derradi<sup>a</sup>, Mayte Bolean<sup>a</sup>, Ana Maria S. Simão<sup>a</sup>, José Luis Millán<sup>b</sup>, Pietro Ciancaglioni<sup>a</sup>, and Ana P. Ramos<sup>a</sup>

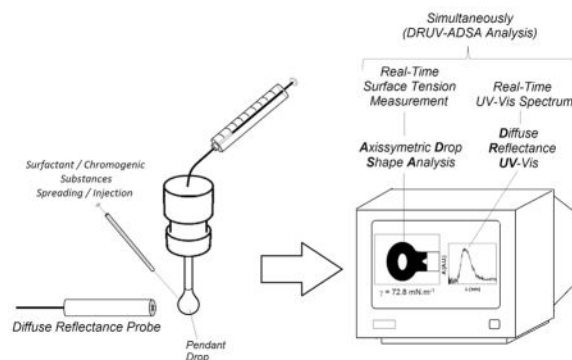
<sup>a</sup>Departamento de Química, Faculdade de Filosofia, Ciências e Letras de Ribeirão Preto, Universidade de São Paulo, 14040-901 Ribeirão Preto, São Paulo, Brazil

<sup>b</sup>Sanford Burnham Prebys Medical Discovery Institute, La Jolla, CA 92037, USA

### Abstract

UV–vis spectroscopy is a powerful tool to investigate surface phenomena. Surface tension measurements coupled to spectroscopic techniques can help to elucidate how the interface organization influences the electronic properties of molecules. However, appreciable sample volumes are usually necessary to achieve strong signals during conduction of experiments. This study reports on the simultaneous acquisition of surface tension data and UV–vis spectra by axisymmetric drop shape analysis (ADSA) coupled to diffuse reflectance (DRUV) spectrophotometry using a pendant microliter-drop that requires small sample volumes and low analyte concentrations. Three example systems gave evidence of the applicability of this technique: (a) disaggregation of an organic dye driven by surfactant as a function of the surface tension and alterations in the UV–vis spectra, (b) activity of a glycosylphosphatidylinositol anchored enzyme estimated from formation of a colored product, and (c) interaction between this enzyme and biomimetic membrane systems consisting of dipalmitoylphosphatidylcholine and cholesterol. Apart from using smaller sample volume, this coupled technique allowed to investigate interfacial organization in the light of electronic spectra obtained *in loco* within a shorter acquisition time. This procedure provided precise interfacial information about static and dynamic systems. This has been the first study describing the kinetic activity of an enzyme in the presence of phospholipid monolayers through simultaneous determination of the surface tension and UV–vis spectra.

### Graphical Abstract



## Keywords

Pendant drop; UV–vis spectroscopy; Interfacial phenomena; Surfactants; Alkaline phosphatase

## 1. Introduction

The surface tension ( $\gamma$ ) of pure liquids or solutions can be measured by many experimental approaches. The pendant drop method relies on axisymmetric drop shape analysis (ADSA) of  $\gamma$  measured at the liquid–air or liquid–liquid interface. Because ADSA uses a microliter sample, this technique is very useful when only a small amount of the target sample is available [1,2]. The traditional methods applied to determine  $\gamma$  usually needs the use of a plate or capillary in contact with the surfaces, thus causing a perturbation at the interface. However, by using ADSA it is possible a  $\gamma$  measurement based in the drop shape, without any external interference. Determination of  $\gamma$  is based on the Laplace equation of capillarity, which relates the pressure across the interface ( $P$ ) with  $\gamma$  and the principal curvature radii ( $R_1$  and  $R_2$ ):

$$\Delta P = \gamma \left( \frac{1}{R_1} + \frac{1}{R_2} \right) \quad (1)$$

This approach allows one to investigate the viscoelastic properties of the surfactant adsorption layer [3] and even to construct a surface pressure ( $\pi$ )–molecular area ( $A$ ) isotherms from insoluble monolayers [4]. Construction of  $\pi$ - $A$  isotherms by traditional techniques that employ Langmuir troughs requires at least milliliters of the liquid subphase and milligrams of the surfactants. However, the use of the pendant microliter-drop as the subphase demands reduced sample volumes and only a very small amount of the surface active compounds. The spread step is crucial for formation of a monolayer at the drop surface [5]:  $\gamma$  depends on the amount of surfactant adsorbed onto a specific drop surface area, so this step will provide specific  $\gamma$  or  $\pi$  values at a certain concentration. In turn,  $\pi$  corresponds to the decrease in  $\gamma$  of the pure aqueous solution ( $\gamma_0$ ) in the presence of the surfactant:

$$\pi = \gamma_0 - \gamma \quad (2)$$

Apart from enabling  $\gamma$  determination, the use of reduced sample volumes is also interesting for other types of analyses, especially when an appreciable analyte concentration is necessary to achieve a considerable signal but small amounts of the analyte are available. The environment of a pendant microliter-drop requires low quantities of the sample because the volumes of the drops are in the order of dozens of microliters.

Another important feature of ADSA is the possibility of coupling simultaneous analysis. The drop can act as a microreactor in which hyphenated techniques aid monitoring of chemical reactions. UV-vis spectrophotometry is a convenient tool to quantify an analyte and to analyze the kinetics or even the dynamics of different systems. The traditional approach uses cuvettes and volumes in the order of milliliters. However, a diffuse reflectance UV-vis (DRUV) probe pointed at the pendant drop in an ADSA apparatus allows one to follow interfacial changes in the systems by spectroscopy. Similarly, McMillan et al. developed a patented technique of UV-vis analysis in the lifecycle of falling drops from the signal tensiortrace of an amplitude-modulated light, also comparing its experimental approach with the traditional UV-vis spectrophotometry [6], and even coupling it to a  $\gamma$  measurement that provides additional interfacial data of surfactant-containing systems [7]. Simultaneous  $\gamma$  and UV-vis analyses using sample volumes in the order of microliters provides an appreciable absorption signal for a low amount of sample. The increased area/volume ratio in a drop ( $\sim 1.5 \text{ m}^2 \text{ L}^{-1}$ ) as compared to the area/volume ratio in a cuvette ( $\sim 0.1 \text{ m}^2 \text{ L}^{-1}$ ) and in the Langmuir trough ( $\sim 0.2 \text{ m}^2 \text{ L}^{-1}$ ) makes the interfacial phenomena become more relevant than the bulk phenomena.

DRUV-ADSA can be applied to study systems where interfacial processes result in spectroscopic changes. More than evidencing processes that occur at the drop microenvironment through UV-vis analysis, DRUV-ADSA also provides data about interfacial activity; allowing the elucidation of possible relations between bulk and surface. Monolayers of insoluble surfactants (such as phospholipids) and micelles of soluble surfactants constitute biomimetic systems. These model systems are widely employed to mimic the interaction of cell membranes with enzymes or other compounds, such as organic dyes used as photosensitizers in photodynamic therapy (PDT) [8,9]. DRUV-ADSA simultaneous analysis also aids investigation into the interaction between micelles and fluorescent dyes. This technique not only gives information about dye disaggregation, but it also reveals the interfacial features of the system through monitoring of the  $\gamma$  of the drop. DRUV-ADSA also allows for enzymatic kinetics monitoring. Spectrophotometric probing of product formation or reactant consumption is the traditional way to perform enzymatic activity analysis. This monitoring can be either discontinuous, by stopping the reaction after a time interval, or continuous, by following the reaction in real time. Enzymes attached to the lipid bilayer of the cell membrane via a glycosylphosphatidylinositol (GPI) anchor display surface activity [10,11]: GPI provides a hydrophobic moiety, whereas the polypeptide chain corresponds to the hydrophilic part. Because these enzymes act as surfactants, it is possible to verify how their interaction with lipid monolayers [12] affects their activity. One of the advantages of the DRUV-ADSA method is that it employs reduced amounts of expensive reactants like proteins and phospholipids. Moreover, this technique allows for simultaneous monitoring of the UV-vis and  $\pi$  or  $\gamma$  alterations in an increased

surface area environment, making changes related to surface adsorption processes more important.

In the present study, three example systems provided evidence of the applicability of the DRUV-ADSA technique: (a) sodium dodecylsulfate (SDS)-induced disaggregation of the organic dye acridine orange (AO), used in photodynamic therapy [13], as a function of  $\gamma$  monitored by the DRUV-ADSA technique; (b) activity of a glycosylphosphatidylinositol anchored enzyme estimated from the formation of a colored product as compared to the traditional UV-vis technique; and (c) interaction between the glycosylphosphatidylinositol anchored enzyme and a biomimetic cell membrane system consisting of dipalmitoylphosphatidylcholine and cholesterol. This has been the first study to describe the kinetic activity of a GPI-anchored enzyme, the tissue-nonspecific alkaline phosphatase (TNAP) [14], in a cell membrane biomimetic system consisting of dipalmitoylphosphatidylcholine-cholesterol through simultaneous determination of  $\gamma$  and absorbance by DRUV-ADSA.

## 2. Materials and methods

### 2.1. Materials

All the solutions were prepared by using dust-free Milli-Q water ( $\gamma = 72.8 \text{ mN m}^{-1}$  and resistivity of  $18.2 \text{ M}\Omega \text{ cm}$ ). Sodium dodecylsulfate (SDS), polyoxyethylene-9-lauryl ether (polidocanol, C12(EO)9), potassium bromide, magnesium chloride, sodium chloride, *p*-nitrophenylphosphate (pNPP), chloroform, 2-amino-2-(hydroxymethyl)propane-1,3-diolhydrochloride (Tris), and 2-amino-2-methyl-propan-1-ol (AMPOL) were purchased from Sigma Chemical Co. [(2*R*)-2,3-Di(hexadecanoyloxy)propyl] 2-(trimethylazaniumyl)ethyl phosphate (dipalmitoylphosphatidyl-choline, DPPC) (99+%) and (8*S*,9*S*,10*R*,13*R*,14*S*,17*R*)-10,13-dimethyl-17-[(2*R*)-6-methylheptan-2-yl] 1,2,6,7,8,9,11,12,14,15,16,17-dodecahydrocyclopenta[*a*]phenanthren-3-one (cholesterol, A-Chol) (99+%) were obtained from AVANTI Polar Lipids. Methanol (MeOH, 99+%) was supplied by J.T. Baker. 3-*N*,3-*N*,6-*N*,6-*N*-tetramethylacridine-3,6-diamine (acridine orange, AO) was acquired from Acros Organic. TNAP was obtained from osteoblasts primary cultures as previously reported elsewhere [15]. Calbiosorb was purchased from Merck-Millipore.

### 2.2. UV-vis spectrophotometry and $\gamma$ analysis

For the traditional UV-vis measurement, the acridine orange (AO) aqueous solution was placed in a quartz cuvette (1.00-cm optical length) and analyzed on an Agilent/HP 8453 UV-vis spectrophotometer. A lab-grade reflection optical fiber probe (Ocean Optics) coupled to a deuterium/halogen light source (DH-2000-BAL Ocean Optics®) and a spectrometer (Ocean Optics® HR 2000) was used to obtain the spectra of the aqueous drop solutions (DRUV). For the DRUV-ADSA coupled experiments, the optical fiber was focused close (around 2–3 mm) to the lateral surface of the drop with volumes varying between 10 and 12  $\mu\text{L}$  with the aid of an automatic tensiometer OCA-20 (Dataphysics), as depicted in Fig. 1. The UV-vis spectra of the aqueous AO solutions was obtained by using pure water as a reference blank for the two experimental approaches.

### 2.3. Interaction between AO and SDS

A 51 mmol L<sup>-1</sup> aqueous AO solution was used to ensure the formation of dimers and to investigate AO disaggregation caused by injection of 0.2 μL of a 3.75 mmol L<sup>-1</sup> SDS aqueous solution inside the drop with the aid of a micro-syringe. Data are reported as the mean ± S.D. of triplicate measurements of different drop preparations.

### 2.4. Preparation of detergent-solubilized TNAP

Solubilized TNAP was prepared according to Simão et al. [15], with slight modifications. Briefly, samples of membrane-bound TNAP (0.2 mg mL<sup>-1</sup>) were solubilized with 1% (w/v, final concentration) polidocanol at 25 °C for 1 h, with constant stirring. After centrifugation at 100,000g for 1 h, 100 μL of solubilized TNAP was incubated with 20 mg of Calbiosorb resin at 4 °C for 2 h, under constant stirring, to obtain TNAP in the absence of any non-ionic surfactant [16].

### 2.5. Kinetic analysis of TNAP in the presence of the phospholipid monolayers

For the enzymatic kinetic analysis, the drops were formed by using a 70 mmol L<sup>-1</sup> aqueous solution of AMPOL pH 10.0, 10 mmol L<sup>-1</sup> pNPP, and 2 mmol L<sup>-1</sup> MgCl<sub>2</sub>. The enzymatic activity was monitored through the changes in the intensity of the UV-vis absorption band around 410 nm, assigned to the formation of *p*-nitrophenolate (pNP<sup>-</sup>), a product of pNPP hydrolysis catalyzed by the injected enzyme.

The specific enzymatic activity was determined by using a correction factor corresponding to the slope of the linear dependence of the DRUV-ADSA absorbance values recorded as a function of the pNP<sup>-</sup> concentration. To this end, the reaction medium containing pNPP was incubated in a traditional cuvette with 1-cm optical length containing 0.528 μg of TNAP. The UV-vis spectra of the product was obtained as a function of time. After 5 min, this same solution was transferred to the DRUV-ADSA apparatus, and the UV-vis spectra was also recorded. The pNP<sup>-</sup> concentration was calculated through the Lambert-Beer law ( $\epsilon^{410\text{nm}} = 17600 \text{ M}^{-1} \text{ cm}^{-1}$  at pH 10), and the specific activity was expressed as a unit (U = nmol of pNP<sup>-</sup> per minute) per mass (mg) of TNAP.

The enzymatic activity and  $\gamma$  were simultaneously measured after injection of 0.5 μL of the 26.4 μg mL<sup>-1</sup> TNAP solution (in the absence of polidocanol) into the drop. The enzymatic activity was also followed in the presence of phospholipids. The monolayers were formed by injection of a few microliters of a chloroformic DPPC/AChol mixture (64:36 molar ratio, final surfactant concentration of 1 mmol L<sup>-1</sup>) inside the drop. Then, 0.2 μL of a 42.7 μg mL<sup>-1</sup> TNAP solution was injected inside the drop, and changes in the UV-vis spectra was registered simultaneously with the changes in  $\gamma$ . The initial time was based upon injection of the enzyme into the system. Data are reported as the mean ± S.D. of triplicate measurements of different drop preparations.

### 3. Results and discussion

#### 3.1. Dynamic experiment: disaggregation of an organic dye

Fig. 2A shows the electronic spectra of AO obtained by using distinct AO concentrations and the conventional UV–vis method. The spectra resembled the spectra obtained by the DRUV-ADSA method (Fig. 2B) at the higher AO concentration. Both spectra presented two absorption maxima close to 470 and 490 nm, as evidenced in the normalized spectra depicted in Fig. 2A. The band at 490 nm was assigned to the individual AO molecules, whereas the band at 470 nm was attributed to formation of AO aggregates [17]. These assignments accounted for the increased absorbance value around 470 nm at higher AO concentration (Fig. 2A).

AO also exhibited a broad fluorescence band between 500 and 650 nm, which explained the negative absorption values between 500 and 600 nm (and also below 440 nm) in the spectrum obtained by DRUV-ADSA. This happened because the optical fiber was not able to discriminate between the light signals that originated from the different phenomena. Fortunately, this did not affect the AO aggregation studies by UV–vis analysis at the drop because only the two maximum absorption wavelengths were necessary.

AO solubilization in 1 mol L<sup>-1</sup> KBr aqueous solutions suppressed the emission band. Indeed, fluorescence quenching by halides is a well-known phenomenon [18,19]. Suppression of the broad fluorescence band around 500–600 nm (inset Fig. 2B) by the halide ion revealed that it was possible to use fluorescent dyes in the microenvironment of a drop during DRUV analysis even when the dye presented low Stokes' shift. The salt solution was not used during the  $\gamma$  measurements—the salt strongly reduced the SDS critical micellar concentration and drastically deformed the shape of the drop, which could affect the UV–vis analysis (which depended on the distance between the DRUV probe and the surface of the drop).

Fig. 2C and D illustrate the simultaneous  $\gamma$  and UV–vis spectrophotometric analyses of the AO solution by DRUV-ADSA after injection of the SDS solution. Equilibrium was achieved around  $\gamma = 40$  mN m<sup>-1</sup>, 2 min after injection of the surfactant. The stabilization of  $\gamma$  coincided with stabilization of the intensity of the absorbance band at 490 nm, related to the presence of non-aggregated AO molecules (Fig. 2C). This possibly indicates that the stationary concentration of AO monomers (a bulk phenomenon) reached after 2 min is dependent of an equilibrium state of the SDS molecules in the bulk and at the drop interface (a surface phenomenon). This interpretation is only possible due to the DRUV-ADSA simultaneous measurement of  $\gamma$  and the absorption values at these specific wavelengths.

At 51 mmol L<sup>-1</sup>, the AO molecules formed a dimeric aggregate. [20]. AO disaggregation reduced the intensity of the absorption band around 468 ( $A_{468 \text{ nm}}$ ) as shown by the ratios in Fig. 2D. Therefore, the ratio between the absorbance intensities  $A_{490 \text{ nm}}/A_{468 \text{ nm}}$  allowed us to follow AO disaggregation. Upon addition of SDS to the AO solution, this ratio increased with time (Fig. 2D), which indicated that the surfactant assisted disaggregation of the AO dimers. There are literature reports on this phenomenon regarding the application of AO in PDT [20], although these studies address only spectral characteristics of the probe. The

interfacial analysis through  $\gamma$  measurement by ADSA proposed herein is an inedited study concerning the AO disaggregation. The linear volume reduction was lower than 4% (inset in Fig. 2D) and did not affect the measurements on this system until about 4 min.

### 3.2. Kinetic experiment: enzymatic activity determination

Fig. 3A and B contain the results concerning standardization of the absorbance values used to determine the specific activity of the enzyme TNAP by DRUV-ADSA. The specific activity determined by the traditional approach (when the sample was placed in a cuvette, Fig. 3A) was  $1474 \pm 15 \text{ U mg}^{-1}$ . This experiment provided the pNP<sup>-</sup> concentrations of the standard curve of the pendant drop shown in Fig. 3B; the correction factor for the absorbance values on the pendant drop was  $7.2 \pm 0.7 \text{ absorbance nmol}^{-1} \text{ L}$ .

Intensification of the absorption band located between 380 and 450 nm, with a maximum at 410 nm, as a function of time (Fig. 4A) evidenced a rise in pNP<sup>-</sup> concentration after TNAP injection into the drop microenvironment. The spectrum obtained by DRUV-ADSA resembled the spectrum achieved by traditional UV-vis (inset in Fig. 4A). The intensity of the band at 410 nm varied linearly as a function of time, as shown in Fig. 4B. The intensity was calculated by correcting the dislocation of the baseline due to the drop evaporation as seen in Fig. 4A.

As shown in Fig. 4B, injection of a few microliters of the TNAP aqueous solution into the drop reduced  $\gamma$  to  $65 \text{ mN m}^{-1}$  at the initial assay time. The linear decrease in  $\gamma$  suggested that TNAP displayed surface activity and corroborated the surface activity of a GPI-anchored protein [21], usually assayed in the presence of non-ionic detergents (detergent-solubilized form) [22] that raises its adsorption at the interface. The surface activity of TNAP calbisorb-treated was achieved at the microenvironment of a pendant drop due to the high area/volume ratio. The polidocanol-free enzyme injected into subphases of higher volumes (results not shown) exhibited no surface activity. Intensification of the band at 410 nm, assigned to pNP<sup>-</sup> formation catalyzed by the enzyme, allowed us to follow the changes in  $\gamma$  simultaneously with the UV-vis measurements (Fig. 4B).

The DRUV-ADSA apparatus proved to be efficient for the continuous analysis of TNAP phosphohydrolytic activity, simultaneously with  $\gamma$  measurement after enzyme injection, as evidenced by the linear pattern of the absorbance values and  $\gamma$  decay as a function of time; both exhibited in Fig. 4B. Modifications in this system, like cofactors concentrations, presence of inhibitors, or presence of surfactants in the microenvironment, enables comparison of possible enzymatic activity changes. Not only activity modulation but also additional data about interfacial phenomena of the enzyme is furnished from DRUV-ADSA, *e.g.* about its migration to the interface due to the presence of salts [23] or regarding the modulation of its surface activity after removal of the GPI anchor [24].

Activity values are usually represented as units of nmol of product per minute of reaction per milligram of enzyme. The standard curve shown in Fig. 3B can help to estimate this specific activity by dividing the absorbance values at the drop by the correction factor of  $7.2 \pm 0.7 \text{ absorbance nmol}^{-1} \text{ L}$ . The specific activity determined with DRUV-ADSA was  $1624 \pm 129 \text{ U mg}^{-1}$ , which resembled the value obtained in the homogeneous environment.

The increase in  $\pi$  ( $\gamma$  reduction) resulting from DPPC/AChol addition to the system augmented the enzymatic activity (Fig. 5A and B and Table 1) possibly because the optimum orientation or accommodation of TNAP at the surface of the system improved substrate accessibility to the active site. The presence of cholesterol in membranes affects incorporation of GPI-bound enzymes (such as TNAP) in cell model systems, hence the choice of a mixed system. It is not the first time that a pendant drop was used as a Langmuir balance after spreading insoluble surfactants on its surface [25]. It is possible to obtain  $\pi$ -A isotherms from amphiphilic lipids using ADSA  $\gamma$  measurement [5].

Caseli et al. [26] used a Langmuir trough to describe the kinetic modulation of TNAP phosphohydrolytic activity by the  $\pi$  values. A sampling microliter tip of a spectrophotometer helped to detect pNP<sup>-</sup> production. The results evidenced that higher  $\pi$ , induced by dimyristoyl phosphatidic acid, culminated in higher enzymatic activity until a discontinuity in the compressional modulus of the monolayer occurred. The DRUV-ADSA approach (volumes around 15  $\mu$ L) requires lower amount of the reactants in order to obtain the same kind of information (migration of TNAP to a liquid-air interface containing amphiphilic lipids structured as a monolayer) achieved in a Langmuir trough (volumes around 100 mL).

Here, raise in  $\pi$  ( $\pi$ ) due to TNAP addition in the presence of the DPPC/AChol monolayers was more pronounced at lower initial  $\pi$  values (Fig. 5A and Table 1), suggesting higher TNAP penetration at this stage. The exclusion  $\pi$  value calculated as  $44 \pm 1 \text{ mN m}^{-1}$  (extrapolated to  $\pi=0$ ; inset in Fig. 5A) evidenced that TNAP insertion at the air-liquid interface induced by the DPPC/AChol was not possible above this value.

Kouzayha et al. [27] also found increased  $\pi$  values in the presence of TNAP at the subphase of a 7-mL Teflon dish containing DPPC monolayers. In the present study, enzyme insertion at the air-liquid interface also diminished at higher  $\pi$ , evidencing that the results obtained by the classic tensiometry and the DRUV-ADSA techniques were compatible.

#### 4. Conclusions

Coupling to a UV-vis portable spectrophotometer improved the pendant drop method of  $\gamma$  analysis and allowed for simultaneous measurement of the surface and photochemical properties of different systems. The high area/volume ratio of the drop favored investigation of interfacial phenomena. This coupled technique, designated DRUV-ADSA, enabled us to investigate interfacial organization in the light of electronic spectra obtained simultaneously *in loco* within reduced acquisition time. This procedure provided precise interfacial information about static, dynamic, and kinetic experiments. A further advantage of DRUV-ADSA was that it required reduced sample volumes and low analyte concentrations, which is beneficial in the case of expensive and little available reactants. Three examples helped to illustrate the versatility of this coupled technique. Sodium dodecylsulfate-induced disaggregation of AO depended on the surfactant concentration and  $\gamma$ . The traditional experimental approach used in other studies containing AO-SDS [20,28] is here represented in a pendant drop microenvironment. The TNAP enzymatic activity determined by the DRUV-ADSA methodology agreed with the value obtained by the conventional UV-vis.



The coupled technique allowed to following continuously the changes in the TNAP activity modulated by the organization of a biomimetic cell model environment. The surface activity of TNAP has been already studied by ADSA [29], however the present study is the first to describe the kinetic activity of the enzyme in the presence of phospholipid monolayers by simultaneous determination of  $\gamma$  and acquisition of UV–vis spectra by DRUV-ADSA. The DRUV-ADSA technique can hereafter be applied to verify the influence of cell membrane models with a variety of compositions in the activity of several enzymes with biological importance.

## Acknowledgments

This study was supported by the Sao Paulo Research Foundation (FAPESP grants 2012/20946-3; 2014/11941-3 and 2015/00345-3) and by the Brazilian National Council of Technological and Scientific Development (CNPq). Ana Ramos and Pietro Ciancaglini are CNPq researchers. The authors thank Professor O.A. Serra for access to the DRUV apparatus.

## Abbreviations

<b>ADSA</b>	axisymmetric drop shape analysis
<b>UV–vis</b>	ultraviolet-visible
<b>DRUV</b>	diffuse reflectance at the UV–vis
<b>PDT</b>	photodynamic therapy
<b>GPI</b>	glycosylphosphatidylinositol
<b>SDS</b>	sodium dodecylsulfate
<b>AO</b>	acridine orange
<b>TNAP</b>	tissue-nonspecific alkaline phosphatase
<b>DPPC</b>	dipalmitoylphosphatidylcholine
<b>AChol</b>	cholestenone
<b>SD</b>	standard deviation
<b>pNPP</b>	<i>p</i> -nitrophenylphosphate
<b>pNP<sup>-</sup></b>	<i>p</i> -nitrophenolate

## References

1. Rotenberg Y, Boruvka L, Neumann AW. Determination of surface tension and contact angle from the shapes of axisymmetric fluid interfaces. *J Colloid Interface Sci.* 1983; 93:169–183.
2. Berry JD, Neeson MJ, Dagastine RR, Chan DYC, Tabor RF. Measurement of surface and interfacial tension using pendant drop tensiometry. *J Colloid Interface Sci.* 2015; 454:226–237. [PubMed: 26037272]
3. Miller R, Sedev R, Schano KH, Ng C, Neumann AW. Relaxation of adsorption layers at solution/air interfaces using axisymmetric drop-shape analysis. *Colloids Surf.* 1993; 69:209–216.

4. Kwok DY, Vollhardt D, Miller R, Li D, Neumann AW. Axisymmetric drop shape analysis as a film balance. *Colloids Surf A Physicochem Eng Aspects*. 1994; 88:51–58.
5. Wege HA, Holgado-Terriza JA, Gálvez-Ruiz MJ, Cabrerizo-Vílchez MA. Development of a new langmuir-type pendant-drop film balance. *Colloids Surf B Biointerfaces*. 1999; 12:339–349.
6. McMillan ND, Smith SRP, Bertho aC, Morrin D, O'Neill M, Tiernan K, et al. Quantitative drop spectroscopy using the drop analyser: theoretical and experimental approach for microvolume applications of non-turbid solutions. *Meas Sci Technol*. 2008; 19:1–18.
7. McMillan ND, O'Rourke B, Morrin D, Pringuet P, Smith SRP, O'Neill M, et al. A new optical method of continuously analysing the surface properties of a single pendant drop while obtaining quality bulk spectral and refractive index measurements of the liquid-under-test. *J Phys Conf Ser*. 2009; 178:1–6.
8. Estevão BM, Pellosi DS, de Freitas CF, Vanzin D, Franciscato DS, Caetano W, et al. Interaction of eosin and its ester derivatives with aqueous biomimetic micelles: evaluation of photodynamic potentialities. *J Photochem Photobiol A Chem*. 2014; 287:30–39.
9. Samanta A, Paul BK, Guchhait N. Studies of bio-mimetic medium of ionic and non-ionic micelles by a simple charge transfer fluorescence probe *N,N*-dimethylaminonaphthyl-(acrylo)-nitrile. *Spectrochim Acta Part A Mol Biomol Spectrosc*. 2011; 78:1525–1534.
10. Ronzon F, Desbat B, Chauvet JP, Roux B. Behavior of a GPI-anchored protein in phospholipid monolayers at the air–water interface. *Biochim Biophys Acta – Biomembr*. 2002; 1560:1–13.
11. Caseli L, Masui DC, Furriel RPM, Leone FA, Zaniquelli MED, Orbulescu J, et al. Rat osseous plate alkaline phosphatase as langmuir monolayer—an infrared study at the air-water interface. *J Colloid Interface Sci*. 2008; 320:476–482. [PubMed: 18280491]
12. Brockman H. Lipid monolayers: why use half a membrane to characterize protein-membrane interactions? *Curr Opin Struct Biol*. 1999; 9:438–443. [PubMed: 10449364]
13. Nafisi S, Saboury AA, Keramat N, Neault JF, Tajmir-Riahi HA. Stability and structural features of DNA intercalation with ethidium bromide, acridine orange and methylene blue. *J Mol Struct*. 2007; 827:35–43.
14. Millán, JL. Wiley VCH Verlag Weinheim. Wiley Online Library; 2006. Mammalian Alkaline Phosphatases: From Biology to Applications in Medicine and Biotechnology.
15. Simão AMS, Yadav MC, Narisawa S, Bolean M, Pizauro JM, Hoylaerts MF, et al. Proteoliposomes harboring alkaline phosphatase and nucleotide pyrophosphatase as matrix vesicle biomimetics. *J Biol Chem*. 2010; 285:7598–7609. [PubMed: 20048161]
16. Camolezi FL, Daghanli KRP, Magalhães PP, Pizauro JM, Ciancaglini P. Construction of an alkaline phosphatase–liposome system: a tool for biomineralization study. *Int J Biochem Cell Biol*. 2002; 34:1091–1101. [PubMed: 12009304]
17. Lyles MB, Cameron IL. Interactions of the DNA intercalator acridine orange with itself, with caffeine, and with double stranded DNA. *Biophys Chem*. 2002; 96:53–76. [PubMed: 11975993]
18. Giri R. Fluorescence quenching of coumarins by halide ions. *Spectrochim Acta Part A Mol Biomol Spectrosc*. 2004; 60:757–763.
19. Joshi NK, Tewari N, Arora P, Rautela R, Pant S, Joshi HC. Photophysical behavior and fluorescence quenching by halides of quinidine dication: steady state and time resolved study. *J Lumin*. 2015; 158:412–416.
20. Wang F, Yang J, Wu X, Wang X, Feng L, Jia Z, et al. Study on the formation and depolymerization of acridine orange dimer in acridine orange-sodium dodecyl benzene sulfonate-protein system. *J Colloid Interface Sci*. 2006; 298:757–764. [PubMed: 16458913]
21. Caseli L, Zaniquelli MED, Furriel RPM, Leone FA. Adsorption of detergent-solubilized and phospholipase C-solubilized alkaline phosphatase at air/liquid interfaces. *Colloids Surf B Biointerfaces*. 2003; 30:273–282.
22. Caseli L, Masui DC, Furriel RPM, Leone Fa, Zaniquelli MED. Incorporation conditions guiding the aggregation of a glycosylphosphatidyl inositol (GPI)-anchored protein in langmuir monolayers. *Colloids Surf B Biointerfaces*. 2005; 46:248–254. [PubMed: 16356698]
23. Langmuir I, Schaefer VJ. Salted-out protein films. *J Am Chem Soc*. 1938; 60:2803–2810.

24. Caseli L, Masui DC, Furriel RPM, Leone FA, Zaniquelli MED. Influence of the glycosylphosphatidylinositol anchor in the morphology and roughness of langmuir–blodgett films of phospholipids containing alkaline phosphatases. *Thin Solid Films*. 2007; 515:4801–4807.
25. Kwok DY, Tadros B, Deol H, Vollhardt D, Miller R, Neumann AW. Axisymmetric drop shape analysis as a film balance: rate dependence of the collapse pressure and molecular area at close packing of 1-Octadecanol monolayers. *Langmuir*. 1996; 12:1851–1859.
26. Caseli L, Oliveira RG, Masui DC, Furriel RPM, Leone FA, Maggio B, et al. Effect of molecular surface packing on the enzymatic activity modulation of an anchored protein on phospholipid langmuir monolayers. *Langmuir*. 2005; 21:4090–4095. [PubMed: 15835979]
27. Kouzayha A, Besson F. GPI-alkaline phosphatase insertion into phosphatidylcholine monolayers: phase behavior and morphology changes. *Biochem Biophys Res Commun*. 2005; 333:1315–1321. [PubMed: 15979580]
28. Ghosh AK, Samanta A, Bandyopadhyay P. Anionic micelle-induced fluorescent sensor activity enhancement of acridine orange: mechanism and pH effect. *Chem Phys Lett*. 2011; 507:162–167.
29. Caseli L, Masui DC, Furriel RPM, Leone FA, Zaniquelli MED. Adsorption kinetics and dilatational rheological studies for the soluble and anchored forms of alkaline phosphatase at the air/water interface. *J Braz Chem Soc*. 2005; 16:969–977.

**HIGHLIGHTS**

- A new approach to simultaneously investigate surface tension and UV–vis spectra was developed.
- The axisymmetric drop shape analysis coupled to diffuse reflectance spectroscopy was used.
- The analysis requires low sample volumes and small analyte concentrations.
- The disaggregation of an organic dye driven by surfactants molecules was followed.
- The activity of an enzyme in the presence of phospholipid monolayers was investigated.

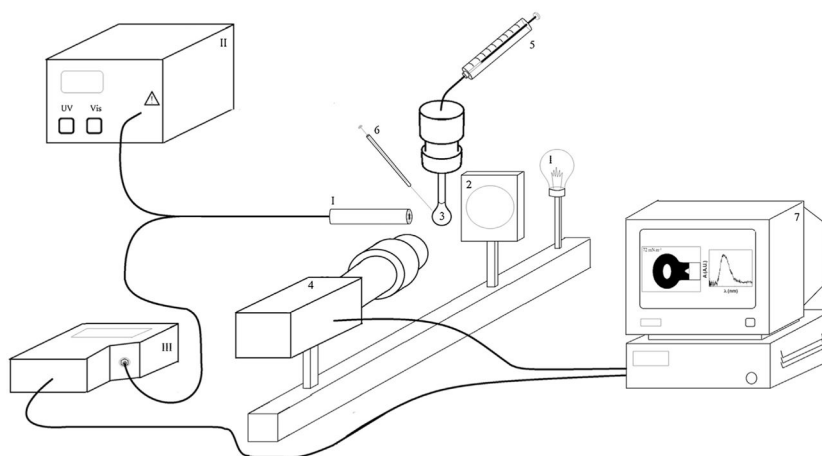


**Fig. 1.** Schematic diagram of the DRUV-ADSA experiments [(1) light source; (2) diffuser; (3) pendant drop; (4) CCD camera; (5) syringe; (6) deposition needle; (7) computer with frame grabber; (I) diffuse reflection probe; (II) deuterium/halogen light source; (III) spectrophotometer].

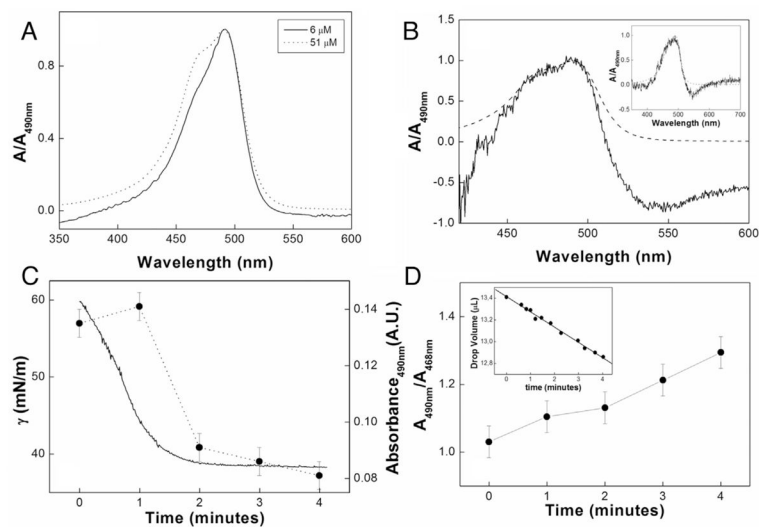


**Fig. 2.**

(A) Spectra of aqueous AO solutions at two different concentrations, recorded in a cuvette, (B) Spectra of  $51 \mu\text{mol L}^{-1}$  aqueous AO solution recorded in a cuvette (dashed line) and in a drop (solid line) (Inset: Spectra of  $51 \mu\text{mol L}^{-1}$  aqueous AO solution recorded in a cuvette (dashed line) or in  $1 \text{ mol L}^{-1}$  KBr aqueous solution in a drop (solid line)), (C)  $\gamma$  vs time for the  $51 \mu\text{mol L}^{-1}$  aqueous AO solution in a drop after injection of SDS (solid line) and the respective absorbance of the drop at 490 nm (●), and (D) ratio between the drop absorbance at 490 and 468 nm (Inset: measurement of the drop volume with time).

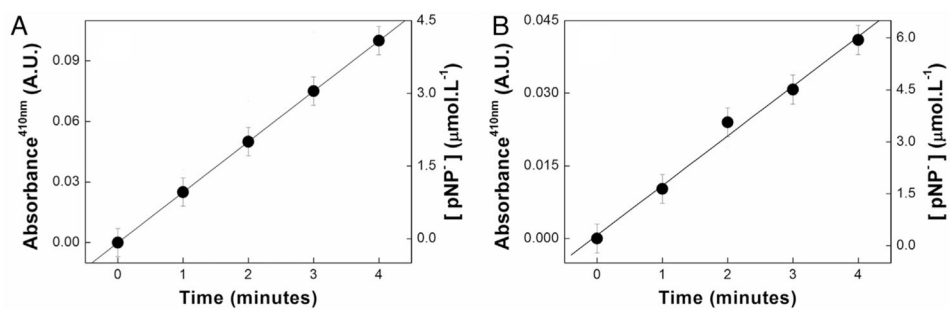


**Fig. 3.** Absorbance and pNP<sup>-</sup> concentrations in the reaction medium containing 0.528 μg of TNAP obtained by traditional spectrophotometry in a cuvette (A) and by DRUV in a pendant drop (B).

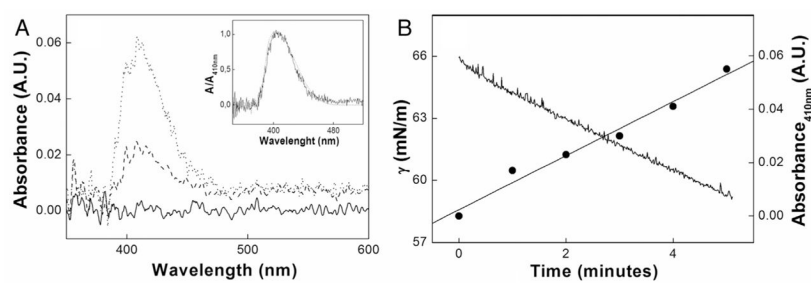


**Fig. 4.** (A) DRUV-ADSA  $pNP^-$  spectra in a drop at 0 (solid line), 2 (dashed line), and 5 (dot line) minutes after TNAP injection (Inset:  $pNP^-$  normalized spectra obtained by traditional (dashed line) and by DRUV-ADSA (solid line) spectrophotometry), (B)  $\gamma$  values after injection of TNAP into the drop (solid line) and simultaneous changes in the intensity of the absorbance band at 410 nm (●).



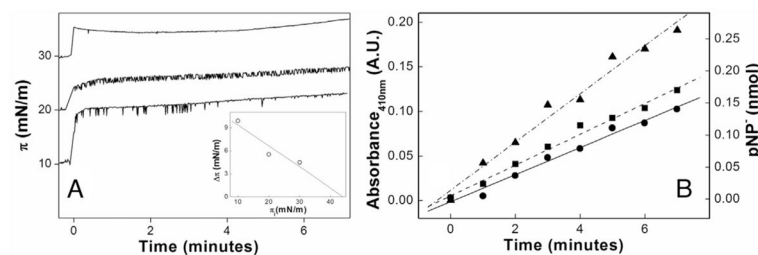


**Fig. 5.**

(A)  $\pi$  measure and (B) amount of pNP<sup>-</sup> produced on the drop at initial  $\pi$  of 10 (●), 20 (■) and 30 mN m<sup>-1</sup> (▲) for the DPPC/Achol monolayers formed on the surface of the drop, after injection of the enzyme. The inset in figure A represents  $\pi$  as a function of the initial surface pressure  $\pi_i$ ; used to calculate the exclusion  $\pi$ .

**Table 1**

Variation in the surface pressure ( $\pi$ ) after addition of the enzyme, and specific phosphomonohydrolase activity of TNAP in the drop determined at different initial  $\pi$  values. See Section 2 for details.

Interface Composition	Initial $\pi$ (mN m <sup>-1</sup> )	$\pi$ (mN m <sup>-1</sup> )	Activity (U mg <sup>-1</sup> )
TNAP	0	4.7 ± 0.2	2646 ± 128
DPPC/AChol + TNAP	10	9.9 ± 0.5	2504 ± 159
DPPC/AChol + TNAP	20	4.9 ± 0.2	3067 ± 169
DPPC/AChol + TNAP	30	4.5 ± 0.2	4321 ± 329

Author Manuscript

Author Manuscript

Author Manuscript

Author Manuscript